Chapter

Adiabatic Shear Band Formation in Metallic Glasses

Shank S. Kulkarni

Abstract

Metallic glasses (MGs) are widely used in many applications due to their unique and attractive properties such as high strength, high elastic limit and good corrosion resistance. Experiments have shown that deformation in MGs is governed by either shear banding or cavitation process leading to a ductile or brittle material response, respectively. In this chapter, shear band formation process in metallic glasses is modeled using free volume theory in infinitesimal deformation. According to the free volume theory, local free volume concentration is considered as order parameter which can be changed by three processes, namely diffusion, annihilation and stress driven creation. Equations are set up for the evolution of free volume and stresses based on conservation of free volume, and mechanical equilibrium, respectively. Another important parameter to consider while modeling the shear bands is temperature as the temperature inside the shear band can reach up to glass transition temperature. This can be achieved by assuming shear band formation process as an adiabatic process whereby evolution equation for temperature is also included with plastic work as the heat source. Example of quasi-static deformation in thin MG strip is solved using this proposed formulation. Formation of the shear band and resulting stresses are studied through the introduction of small inhomogeneity along the thickness direction in the strip.

Keywords: metallic glasses, shear bands, adiabatic process, free volume theory, inhomogeneous deformation

1. Introduction

The basic difference between any conventional metal and metallic glass (MG) is their arrangement of atoms in the solid state. When any solid is cooled below its melting point it tries to arrange in the crystalline lattice which is the structure with minimum energy. Atoms of every conventional metal arrange themselves in this crystalline manner just below the melting point and this process is very quick. On the other hand, glass takes a lot more time to arrange in a crystalline manner and glass liquid can be cooled below melting point before glass transition temperature is reached. Due to which atoms in glass remain in a random position and do not have any preferential arrangement.

Earlier, Turnbull and Cech [1, 2] predicted that by rapid cooling, crystallization can be suppressed. In the late 1960s, it was discovered by Jun et al. [3] at California Institute of Technology that it is possible to keep atoms of metal in random packing in the solid state either by increasing the time required to form crystal or by cooling

the liquid so fast that there will not be sufficient time to form the crystal. By this method, the liquid solidifies as MG, which is metal without any particular arrangement of atoms. When Jun et al. [3] performed their classic experiment of rapid-quenching on Al-Si alloys MGs came to reality. MGs are opaque, shiny, smooth, gray in color and less brittle than conventional glass. Yield strength of MGs is reported to be as high as 1.9 GPa [4] and is found to be more resistant to fracture than ceramics. As there are no grain boundaries in MGs they are resistant to corrosion and wear. They have high electrical sensitivity which leads to low eddy current losses. Also, MGs formed from alloys of Fe, Co, or Ni has soft magnetic properties as well.

In spite of all the attractive properties, commercial use of MGs was not possible until the 1990s. This is due to the fact that it was not practically possible to attain required cooling rate (10^{6}°C/s) so that there will not be any time for crystallization [4]. Even if the cooling rates were attained, the thickness of MGs that was cast was very small because of slow heat conduction. The main focus was on how to decrease the cooling rate and simultaneously increase the casting thickness. Finally, researchers found that if a different metal alloy is added to the liquid metal, then the amorphous structure can be achieved at lower cooling rates. Presence of more number of elements increases the size and complexity of the unit cell which leads to amorphous formation. If there is a large difference between sizes of a radius of different atoms then packing density increases which again favors amorphous arrangement. Using this technique, around 1990, first commercial MG was developed and named "Vitreloy," also known as Liquidmetal [4]. Following the success of "Vitreloy," there was tremendous development in reducing the critical cooling rate (minimum rate to suppress the formation of crystalline lattice). Due to the increase in the achievable thickness (>1 cm) of MGs, they are also known as bulk metallic glasses (BMGs) [5]. A large variety of BMGs is found out using different alloys in varying proportions.

1.1 Applications of MGs

MGs are used in golf club heads, baseball bats and tennis rackets due to low damping and ability to transfer a large fraction of impact energy to the ball. Its high strength to weight ratio allows the mass to be distributed differently, which means different shapes can be achieved for club heads. They are also used in bicycle frames, hunting bows, fishing equipment and guns.

As a result of being very good corrosion and wear resistant, use of MGs in luxurious items is increasing day by day. Also, they have excellent scratch resistance along with smooth and shiny surface which makes them ideal for watch cases, spectacle frames, rings, pens and mobile cases.

MGs are biocompatible with a non-allergenic form which allows using it as a knee-replacement device or pacemaker casing. Also, they are used in surgical blades as they are less expensive than diamond blades as well as sharper and long-lasting than steel. Due to the lack of grain structure, a blade can be sharpened to an exceptional edge. They can also be used in razor blades and knives.

Micro electro mechanical systems offer a very wide range of application for MGs. They are used in micromirrors used in digital light processor (DLP) technology for data projectors. MGs are lighter, stronger and easily molded due to which they are used in components of liquid crystal display (LED), ultra-personal computer screens and casing of cameras. Also, high hardness and lack of grain structure allow it to use as information storage of digital data.

1.2 Deformation mechanism

Fracture toughness of MGs exhibits a very wide range from 1 to 140 MPa $\sqrt{m}$ [6]. Lewandowski et al. [7] found that the fracture toughness can be correlated with Poisson's ratio. As Poisson's ratio decreases fracture energy decreases resulting in brittle fracture. Brittle fracture surface shows very fine corrugations of the length scale of nanometers on the other hand ductile fracture surface shows a coarse pattern with deep impressions of the length scale of micrometers. Thus higher Poisson's ratio implies higher fracture toughness and a critical Poisson's ratio around 0.34 is found for the transition between brittle and ductile behavior [8]. In order to understand the effect of Poisson's ratio on the deformation mechanism of MGs, Murali et al. [8] conducted atomic scale simulations on two MGs, *FeP* and *CuZr* with Poisson's ratio 0.33 and 0.39, respectively. They found that *FeP* with Poisson's ratio 0.33 fractures in brittle fashion according to cavitation mechanism. Cavitation is the process of nucleation of voids inside a solid. In brittle fracture, the crack propagates by continuous series of nucleation of voids in front of the crack tip. This nucleation of void takes place in void-free solid when hydrostatic stress at any point reaches a critical value known as cavitation stress σ_c. Firstly, single void nucleates and grows and after sufficient growth of the void, next one nucleates at some distance from the new crack tip and crack propagation continuous. On the other hand, in *CuZr* with Poisson's ratio 0.39 instead of the propagation of crack tip, they observed blunting of the crack tip. Shear bands were formed near the crack tip as the applied strain was increased. This extensive shear banding near crack tip gives rise to ductile failure at large strains. There could be a large amount of dissipation of energy inside shear bands which can cause localized melting observed on the ductile fracture surface.

Hence two different type of fracture mechanism were observed depending on Poisson's ratio. Brittle MGs shows crack propagation while ductile shows crack blunting with extensive shear banding. In this chapter, the focus will be on the modeling of shear bands causing ductile failure.

1.3 Microscopic deformation models

A large amount of research has been done to understand the nature of mechanism which causes shear band, but still, it is not totally clear. Gilman [9, 10] modeled shear bands in MGs in terms of glide of dislocations. After that Chaudhari et al. [11] and Shi [12] investigated the stability of dislocations in MGs but results did not follow the results came from theoretical work. They found that both edge and screw dislocations are rather stable. Recently Takeuchi and Edagawa [13] did some atomic simulations to review so far proposed deformation models and to understand deformation induced softening, shear band formation and its development.

In the late 1970s, two classic theories were developed for the understanding of deformation in case of MGs assuming that the fundamental process responsible for deformation is a local arrangement of atoms which accommodates the local shear strain. The first theory is known as the shear transformation zone model by Argon. This model depends on the shear transformation zone (STZ) which is a local cluster of atoms undergoing plastic shear distortion. Argon [14] was first to develop a model of STZ where he treated the problem as an Eshelby inclusion. When MGs undergoes uniform stress STZ will be selected on the basis of energies which in turn must be dependent upon local atomic arrangements.

The second theory was developed by Spaepen which was based on the free volume model. The basic free volume model was developed by Turnbull [15, 16] and later on applied to the MGs by Spaepen [17]. This model is based on free volume concentration as an order parameter which is nothing but extra volume where atom can move freely. The distribution of free volume controls the deformation in MGs and regions having more free volume would localize the shear deformation. Deformation in MGs is considered a series of atomic jumps which in addition to temperature can be driven by applied shear stress.

This model was applied to study inhomogeneous deformation during shear load by Taub and Spaepen [18], Steif et al. [19], where they assumed a band of slightly weaker material in their analysis where strain can be localized. Vaks [20] proposed the mechanism for the origin of shear bands in amorphous alloys. Vaks supposed that the localized plastic flow is connected with the preceding formation of weakened band region in which free volume is increased. Huang et al. [21] developed a general theory for modeling of inhomogeneous deformation by considering it as the isothermal process and solved 1D simple shear problem as an example. They showed that initial inhomogeneity of free volume increases with applied strain and cause localization of strain in that region leading to the creation of the shear band. Kulkarni and Bhandakkar [22] extend this theory to finite deformation. Gao [23] extended the above idea and solved 2D plate problem for inhomogeneous deformation still treating the deformation as the isothermal process. Evolution of free volume concentration during high-temperature deformation was studied by De Hey et al. [24], Yang et al. [25, 26] and Lewandowski and Greer [27] found a temperature rise of 0.25°C in a hot band of about 0.4 mm width signifying the importance of thermo-mechanical model for modeling of shear bands. Then Gao et al. [28] solved homogeneous deformation case of simple shear by considering deformation as an adiabatic process where plastic work was done was considered a source of heat. Jiang and Dai [29] using the approach of Steif et al. [19] have shown that initial formation of shear band depends dominantly on the free volume concentration but after yield point temperature also plays an important role and initial slight distribution of free volume concentration can lead to significant strain localization resulting a shear band. Ruan et al. [30] investigated the physical origin of the shear band by assuming that instability is due to bifurcation of the constitutive model at a particular stress state. They established a new constitutive model based on the rugged free energy landscape of MGs.

In addition to continuum models, beam theory has also been used to model deformation in MGs. Conner et al. [31] modeled the experimentally observed inverse dependence of ductility to plate thickness by treating the shear band as mode II crack and calculating the conditions for their formation when subjected to plane strain bending. Ravichandran and Molinari [32] treated the beam as elastic-plastic with yielding based on Tresca yield criteria and included shear band dissipation. They studied the shear banding phenomenon in thin plates of MGs subjected to plane strain banding. Dasgupta et al. [33] explains the mechanism of shear bands on the basis of considering the shear band as an Eshelby inclusion. They found out that under compressive test, Eshelby inclusions in MGs arrange themselves in a line which is at 45° to the compressive stress and in this process energy is minimized.

Apart from above, Murali et al. [8] showed that in case of brittle MGs deformation occurs through cavitation mechanism, on that basis to explain that behavior, Singh et al. [34] propose a model of a heterogeneous solid containing a distribution of weak zone. Huang et al. [35] also presented a theoretical description of void growth undergoing hydrostatic tension. They found out that cavitation instabilities prefer to occur in solid with higher pressure sensitivity coefficient. Schuh et al. [36]

and Greer et al. [37] gives a comprehensive review of recent advances in understanding the mechanical behavior of MGs, with particular emphasis on the deformation and fracture mechanics.

2. General formulation for infinitesimal deformation

2.1 Governing equations and constitutive laws

Assuming no body force, governing equations for quasi-static deformation in isotropic and homogeneous materials are [38]:

$$\sigma_{ij,j} = 0 \tag{1}$$

Under small deformation regime, strain displacement relation is given by

$$\varepsilon_{ij} = \frac{1}{2}\left(u_{i,j} + u_{j,i}\right) \tag{2}$$

where $i, j = 1, 2, 3$ and $()_j$ means differentiation with respect to jth spatial coordinate. σ_{ij} are components of Cauchy stress tensor, u_i are the components of displacement, ε_{ij} are components of strains. For MGs, strain is decomposed as [21],

$$\varepsilon_{ij} = \varepsilon^e_{ij} + \varepsilon^p_{ij} + \frac{1}{2}(\xi - \xi_0)\delta_{ij} \tag{3}$$

where, ε^e_{ij} is the elastic strain, ε^p_{ij} is the deviatoric plastic strain and, $(\xi - \xi_0)$ is the inelastic dilatation strain (strain due to excess free volume), where ξ is local concentration of free volume and ξ_0 is the free volume concentration at the reference state with no strain. Dividing the stress tensor into mean stress and deviatoric stress tensor,

$$\sigma_m = \frac{1}{3}(\sigma_{11} + \sigma_{22} + \sigma_{33}) \tag{4}$$

$$S_{ij} = \sigma_{ij} - \sigma_m\delta_{ij} \tag{5}$$

The Mises effective shear stress is

$$\tau_e = \sqrt{\frac{1}{2}S_{ij}S_{ij}} \tag{6}$$

Elastic strain and stress are relates to each other by Hooke's law,

$$\sigma_{ij} = 2\mu\left(\varepsilon^e_{ij} + \frac{\nu}{1-2\nu}\varepsilon^e_{kk}\delta_{ij}\right) \tag{7}$$

where μ is shear modulus and ν is Poisson's ratio.

Following Mises theory [39] flow of deviatoric plastic strain ε^p_{ij} is assumed to be in the same direction as deviatoric stress tensor S_{ij}, with its rate depending upon concentration of free volume ξ_f, effective shear stress τ_e and mean stress σ_m as:

$$\frac{\partial\varepsilon^p_{ij}}{\partial t} = f\left(\xi_f, \tau_e, \sigma_m\right)\frac{S_{ij}}{2\tau_e} \tag{8}$$

The inelastic dilatation strain is associated with change of concentration of free volume. This change of concentration of free volume depends upon local concentration free volume itself ξ_f, effective shear stress τ_e and mean stress σ_m [21].

$$\frac{\partial \xi_f}{\partial t} = D\xi_{,ii} + g\left(\xi_f, \tau_e, \sigma_m\right) \tag{9}$$

where D is diffusivity which is assumed to be only dependent on temperature.

2.2 Flow equation

Irreversible part of strain rate that is plastic strain rate can be represented by flow rule as,

$$\frac{\partial \gamma^p}{\partial t} = 2\vartheta \exp\left(-\frac{\alpha\vartheta^*}{\xi_f}\right) \exp\left(-\frac{\Delta G^m}{k_B T}\right) \sinh\left(\frac{\tau\Omega}{2k_B T}\right) \tag{10}$$

The above flow rule is based on the microscopic model for the shear strain rate in amorphous metals proposed by Spaepen [17]. By assuming that shear strain rate depends on three quantities as,

$$\begin{aligned}\dot{\gamma} = &(\text{strain produced at each jump site}) \times (\text{fraction of potential jump site}) \\ &\times (\text{net number of forward jumps at each site per second})\end{aligned} \tag{11}$$

A potential site is a region in which the free volume is greater than some critical volume. The shear strain at each potential jump site is assumed to be 1. Fraction of potential jump site is the probability that any atom has free volume greater than critical free volume. Since MGs have amorphous structure of atoms probability is calculated by statistical distribution. Therefore the fraction of potential jump sites is $\exp\left(-\alpha\vartheta^*/\xi_f\right)$, where α is geometrical factor of order 1, ϑ^* is critical volume and ξ_f is average free volume per atom.

By rate theory when there is no shear stress applied net number of forward jumps and backward jumps should be equal to each other and number of successful jumps per second will be equal to $\vartheta \exp\left(-\Delta G^m/k_B T\right)$, where ϑ is the frequency of atomic vibration, ΔG^m is activation energy, k_B is Boltzmann's constant and T is absolute temperature.

When shear stress is applied, shear strain allows to lower potential energy in one direction and hence system becomes biased. Due to this one more factor to be added to above equation. So net rate of forward jumps is,

$$= 2\vartheta \exp\left(-\frac{\Delta G^m}{k_B T}\right) \sinh\left(\frac{\tau\Omega}{2k_B T}\right) \tag{12}$$

where Ω is the atomic volume and τ is the shear stress.

2.3 Free volume change rate

Free volume is the excess volume where atoms can freely move. This is defined as the difference between average atomic volume and average atomic volume in an

ideally ordered structure. Stress-driven creation, annihilation and diffusion are the three processes by which local free volume concentration can be changed.

At sufficiently high stress an atom can be squeezed into a neighboring hole with a smaller volume. Due to this neighboring atom of new positions get displaced by some amount creating new free volume. Opposite to that annihilation process tries to reduce the total free volume and restore the system to the initial state. On the other hand diffusion process neither creates nor destroys free volume, but try to just redistribute it until it is uniformly distributed everywhere. Therefore the net rate of increase of free volume is must be the difference between the rate of creation of free volume and rate of the annihilation of free volume and is given as [17],

$$\dot{\xi}_f = \vartheta^* \vartheta \exp\left(-\frac{\alpha\vartheta^*}{\xi_f}\right) \exp\left(-\frac{\Delta G^m}{k_B T}\right) \left[\frac{2\alpha k_B T}{\xi_f \mu^*} \left\{\cosh\left(\frac{\tau\Omega}{2k_B T}\right) - 1\right\} - \frac{1}{n_D}\right] \quad (13)$$

where n_D is number of atomic jumps required to annihilate free volume equal to ϑ^* and

$$\mu^* = \frac{2}{3}\mu \frac{1+\nu}{1-\nu} \quad (14)$$

By comparing Eqs. (10) and (13) with Eqs. (8) and (9), respectively,

$$f\left(\xi_f, \tau_e\right) = 2\vartheta \exp\left(-\frac{\alpha\vartheta^*}{\xi_f}\right) \exp\left(-\frac{\Delta G^m}{k_B T}\right) \sinh\left(\frac{\tau\Omega}{2k_B T}\right) \quad (15)$$

$$g\left(\xi_f, \tau_e\right) = \vartheta^* \vartheta \exp\left(-\frac{\alpha\vartheta^*}{\xi_f}\right) \exp\left(-\frac{\Delta G^m}{k_B T}\right) \left[\frac{2\alpha k_B T}{\xi_f \mu^*} \left\{\cosh\left(\frac{\tau\Omega}{2k_B T}\right) - 1\right\} - \frac{1}{n_D}\right] \quad (16)$$

It can be seen from the above equations that the functions f and g are independent of mean stress σ_m.

2.4 Temperature evolution equation

In MGs width of the shear band is in the order of 10–20 nm. Heat gets generated from plastic work done during shear banding. Yang et al. [25] have shown that 0.4 mm wide shear band can cause a temperature rise of about 0.25°C. As width decreases temperature rise increases because there is less space for heat to be dissipated. Also, thermal conductivity is less for MGs [40, 41], so temperature rise in shear bands can cause the glass to reach its glass transition temperature [42]. Hence it is needed to account for the heat induced in the shear band while modeling them in MGs.

Following Yang [23, 25, 26] thermal transport equation is given as,

$$\rho C_p \frac{\partial T}{\partial t} = k_0 \frac{\partial^2 T}{\partial x^2} + \alpha_{TQ} \sigma_{ij} \frac{\partial \varepsilon_{ij}^p}{\partial t} \quad (17)$$

where ρ is material density, C_p is the specific heat, k_0 is thermal conductivity and α_{TQ} is Taylor-Quinney coefficient which represents the fraction of plastic work converted to heat. Coefficient of thermal expansion for metallic glasses is very small; therefore thermal strain is not comparable with total strain hence it is neglected in this case.

2.5 Viscosity

Combining Eq. (10) and definition of stress driven viscosity [19],

$$\eta_v = \frac{\tau}{\dot{\gamma}^p} = \frac{\tau}{2\sinh\left(\frac{\tau\Omega}{2k_BT}\right)}\vartheta^{-1}\exp\left(-\frac{\alpha\vartheta^*}{\xi_f}\right)\exp\left(-\frac{\Delta G^m}{k_BT}\right) \tag{18}$$

Hence change in free volume changes viscosity in exponential manner. Therefore as free volume increases viscosity decreases and softening occurs.

3. One-dimensional shear problem

Figure 1 shows the geometry of thin strip of width $2h$ subjected to constant shear strain.

The dimensions of the strip in the direction normal to width are very large compared to h and hence assumed infinity. Shear strain rate is assumed to be very low so that it is under quasi-static range. Shear stress will lead to the creation of more free volume and the strip will dilate. If this creation of free volume is not uniform across the width of the layer, then due to geometric constraints there will be equal normal stresses in y and z direction. There is no restriction on the material to dilate along x direction, as normal stress is zero in this direction. In this case, effective shear stress is given by

$$\tau_e = \sqrt{\tau^2 + \frac{1}{3}\sigma^2} \tag{19}$$

Also in this case shear strain decomposition can be written as

$$\dot{\gamma} = \dot{\gamma}^e + \dot{\gamma}^p \tag{20}$$

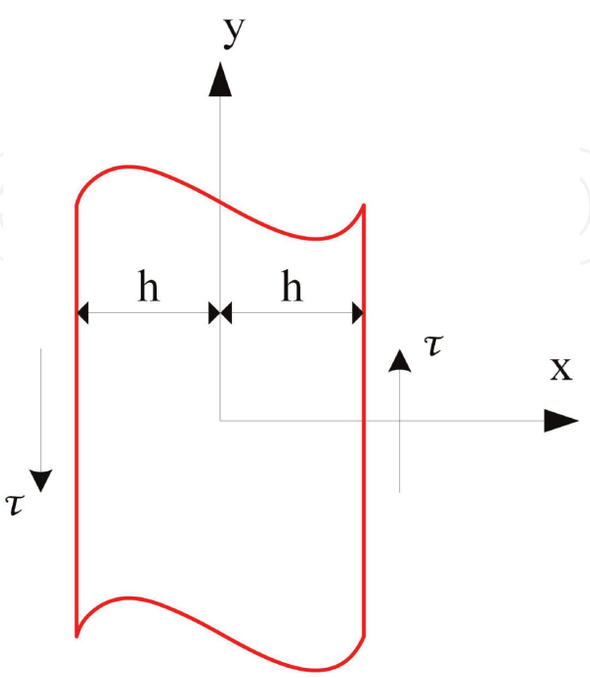

Figure 1.
Shear problem geometry.

Using Eq. (8) for plastic shear strain rate and using Hook's law Eq. (20) becomes

$$\frac{\partial \gamma}{\partial t} = \frac{1}{\mu}\frac{d\tau}{dt} + f\left(\xi_f, \tau_e\right)\frac{\tau}{\tau_e} \tag{21}$$

In the absence of any normal force acting on strip, force balance equation in x-direction gives,

$$\int_{-h}^{h} \sigma(x,t)dx = 0, \tag{22}$$

and the average shear strain rate is

$$r = \frac{1}{2h}\int_{-h}^{h} \frac{\partial \gamma}{\partial t}dx \tag{23}$$

Therefore by integrating both sides of Eq. (21) with respect to x from $-h$ to h gives us

$$\frac{d\tau}{dt} = \mu\left[r - \frac{1}{2h}\int_{-h}^{h} f\left(\xi_f, \tau_e\right)\frac{\tau}{\tau_e}dx\right] \tag{24}$$

Applying Eq. (3) for normal strain ε in x direction gives,

$$\frac{\partial \varepsilon}{\partial t} = \frac{(1-2\nu)}{2\mu}\frac{d\sigma}{dt} + f\left(\xi_f, \tau_e\right)\frac{\sigma}{6\tau_e} + \frac{1}{3}\frac{\partial \xi_f}{\partial t} \tag{25}$$

Integrating above Eq. (25) and by eliminating term of integration normal stress over width by using Eq. (22),

$$\frac{\partial \varepsilon}{\partial t} = \frac{1}{2h}\int_{-h}^{h}\left[f\left(\xi_f, \tau_e\right)\frac{\sigma}{6\tau_e} + \frac{1}{3}\frac{\partial \xi_f}{\partial t}\right]dx \tag{26}$$

Free volume concentration is assumed to be changing only in x direction and uniform along y and z direction. Then Eq. (9) becomes as,

$$\frac{\partial \xi_f}{\partial t} = D\frac{\partial^2 \xi_f}{\partial x^2} + g\left(\xi_f, \tau_e\right) \tag{27}$$

Lastly, assuming that temperature also can vary only in x direction, Eq. (17) becomes,

$$\rho C_p \frac{\partial T}{\partial t} = k_0 \frac{\partial^2 T}{\partial x^2} + \alpha_{TQ}\tau\dot{\gamma}^p \tag{28}$$

Normalization of equations is done so that to get clearer picture and to deal with dimensionless quantities. Normalization is done as; stresses by shear modulus μ, free volume concentration by ϑ^*, time by $(1/R)$, temperature by the room

temperature T_0 and space x by l [21, 43, 44]. Normalized shear stress, free volume concentration, time, temperature and space are denoted by $\hat{\tau}$, ξ, $\hat{t}$, $\hat{T}$, and $\hat{x}$, respectively, where R is,

$$R = \vartheta \exp\left(-\frac{\Delta G^m}{k_B T}\right) \tag{29}$$

3.1 Isothermal homogeneous deformation

Here Eqs. (24) and (27) are applied to the case of homogeneous deformation. Free volume concentration is uniform throughout the width of strip. Hence normal stress will be zero and so the effective shear stress is equal to the shear stress. ($\tau_e = |\tau|$).

So Eq. (24) becomes,

$$\frac{d\tau}{dt} = \mu\left[r - f\left(\xi_f, \tau_e\right)\right] \tag{30}$$

and Eq. (27) becomes

$$\frac{\partial \xi}{\partial t} = g\left(\xi_f, \tau_e\right) \tag{31}$$

After normalization, Eqs. (30) and (31) are,

$$\frac{d\hat{\tau}}{d\hat{t}} = \frac{r}{R} - 2\exp\left(-\frac{\alpha}{\xi}\right)\sinh\left(\hat{\tau}\overline{\mu}\right) \tag{32}$$

$$\frac{\partial \xi}{\partial \hat{t}} = \exp\left(-\frac{\alpha}{\xi}\right)\left[\frac{\alpha}{\beta\overline{\mu}\xi}\left\{\cosh\left(\hat{\tau}\,\overline{\mu}\right)\right\} - \frac{1}{n_D}\right] \tag{33}$$

where $\overline{\mu} = \mu\Omega/(2k_B T)$.

Equations (32) and (33) are solved numerically using fourth order Runge-Kutta scheme for shear strain rate r = 0.2 s^{-1} to see variation of shear stress and free volume concentration with respect to time [45]. Here Vitreloy 1 BMG is taken as a model material. Mechanical properties and parameters for Vitreloy 1 are given in **Table 1**. **Figure 2** shows the evolution of free volume and shear stress with shear strain. Initial free volume concentration is 0.0075 and initial stress is zero.

Properties and parameters	Notation	Value
Shear modulus	μ	49.68 GPa
Poisson's ratio	ν	0.3
Density	ρ	6810 kg/m^3
Specific heat	C_p	330 J/kgK
Activation energy	ΔG^m	0.2–0.5 eV
Average atomic volume	Ω	20 A^3
Thermal conductivity	k	20 W/mK
Taylor-Quinney coefficient	α_{TQ}	0.9
Free volume diffusivity	D	2×10^{-16}

Properties and parameters	Notation	Value
Frequency of atomic vibration	ϑ	10^{13} s^{-1}
Room temperature	T_0	300 K
Length	l	9.4 μm
Geometrical factor	α	0.15
Atomic jumps to annihilate free volume of ϑ^*	n_D	3
Average applied strain rate	r	0.2 s^{-1}
Initial free volume concentration	ξ_i	0.0075

Table 1.
Mechanical properties and parameters for Vitreloy 1 [25, 31, 32].

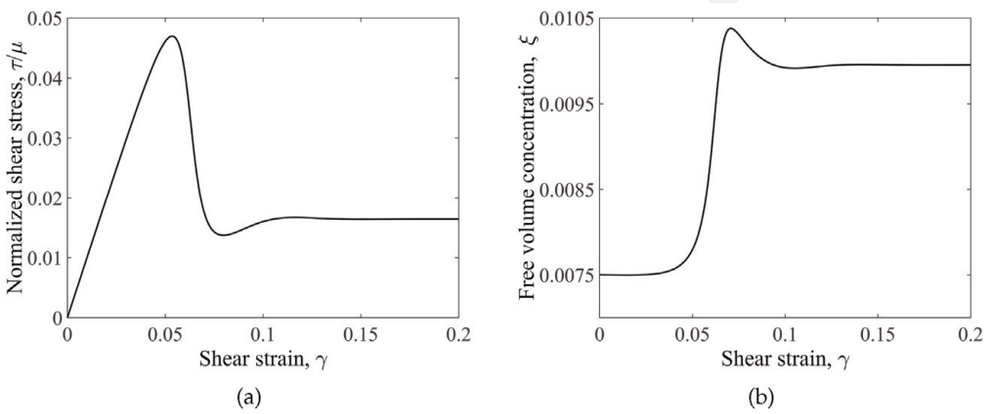

Figure 2.
Results for 1D shear problem with isothermal homogeneous deformation. (a) Normalized shear stress versus shear strain, and (b) free volume concentration versus shear strain.

From **Figure 2**, initially, shear stress increases linearly with shear strain solely due to elastic deformation in the strip. After some time increased shear stress creates more and more free volume so that free volume concentration increases rapidly which eventually leads to softening of the material. This softening corresponds to a sharp turn in the stress-strain diagram of **Figure 2a** and shear stress continues to decrease afterward. This decay of shear stress now retards the creation of free volume and finally, the system gets stabilized and steady state is achieved. At steady state both free volume concentration and shear stress are constant and MG acts like a liquid. The value of peak stress and final free volume concentration at steady state depends upon material parameters and applied strain rate.

3.2 Adiabatic homogeneous deformation

In the previous section, shear band formation is considered as an isothermal process but in reality, there is very little time for the entire heat produced by friction to flow out. Therefore to take care of that it is better to consider shear banding as an adiabatic process. Therefore thermal transport equation should also be considered.

For homogeneous case there is no temperature variation over the width of strip and plastic work is solely due to shear stress. Therefore Eq. (28) will reduce to,

$$\rho C_p \frac{dT}{dt} = \alpha_{TQ} \tau \dot{\gamma}^p \tag{34}$$

After normalizing Eq. (34), it will become as

$$\frac{d\hat{T}}{d\hat{t}} = \frac{\mu}{T_0}\frac{\alpha_{TQ}}{\rho C_p}\left(\hat{\tau}\frac{d\dot{\gamma}^p}{d\hat{t}}\right) \tag{35}$$

Also for adiabatic case Eqs. (24) and (27) will become as

$$\frac{d\hat{\tau}}{d\hat{t}} = \frac{1}{R}\left[r - 2\vartheta \exp\left(-\frac{\alpha}{\xi}\right)\exp\left(-\frac{\Delta G^m}{k_B T_0 \hat{T}}\right)\sinh\left(-\frac{\hat{\tau}\,\overline{\mu}}{\hat{T}}\right)\right] \tag{36}$$

$$\frac{\partial\xi}{\partial\hat{t}} = \frac{1}{R}\vartheta \exp\left(-\frac{\alpha}{\xi}\right)\exp\left(-\frac{\Delta G^m}{k_B T_0 \hat{T}}\right)\left[\frac{\alpha\hat{T}}{\beta\overline{\mu}\xi}\left\{\cosh\left(-\frac{\hat{\tau}\,\overline{\mu}}{\hat{T}}\right) - 1\right\} - \frac{1}{n_D}\right] \tag{37}$$

Using numerical integration, Eqs. (35)–(37) are solved for variation of shear stress, free volume concentration and temperature with respect to applied strain for same initial conditions and strain rate.

Figure 3 shows the result of numerical solution of Eqs. (35)–(37). In **Figure 3a** and **b**, results are compared with the case of isothermal homogeneous deformation, where dash lines indicate the isothermal model and solid lines are for adiabatic model. When applied shear strain is small glass strip is in an elastic state. In this state, both results are nearly the same because plastic work causes temperature rise and in an elastic state plastic work is negligible. More and more increase in stress

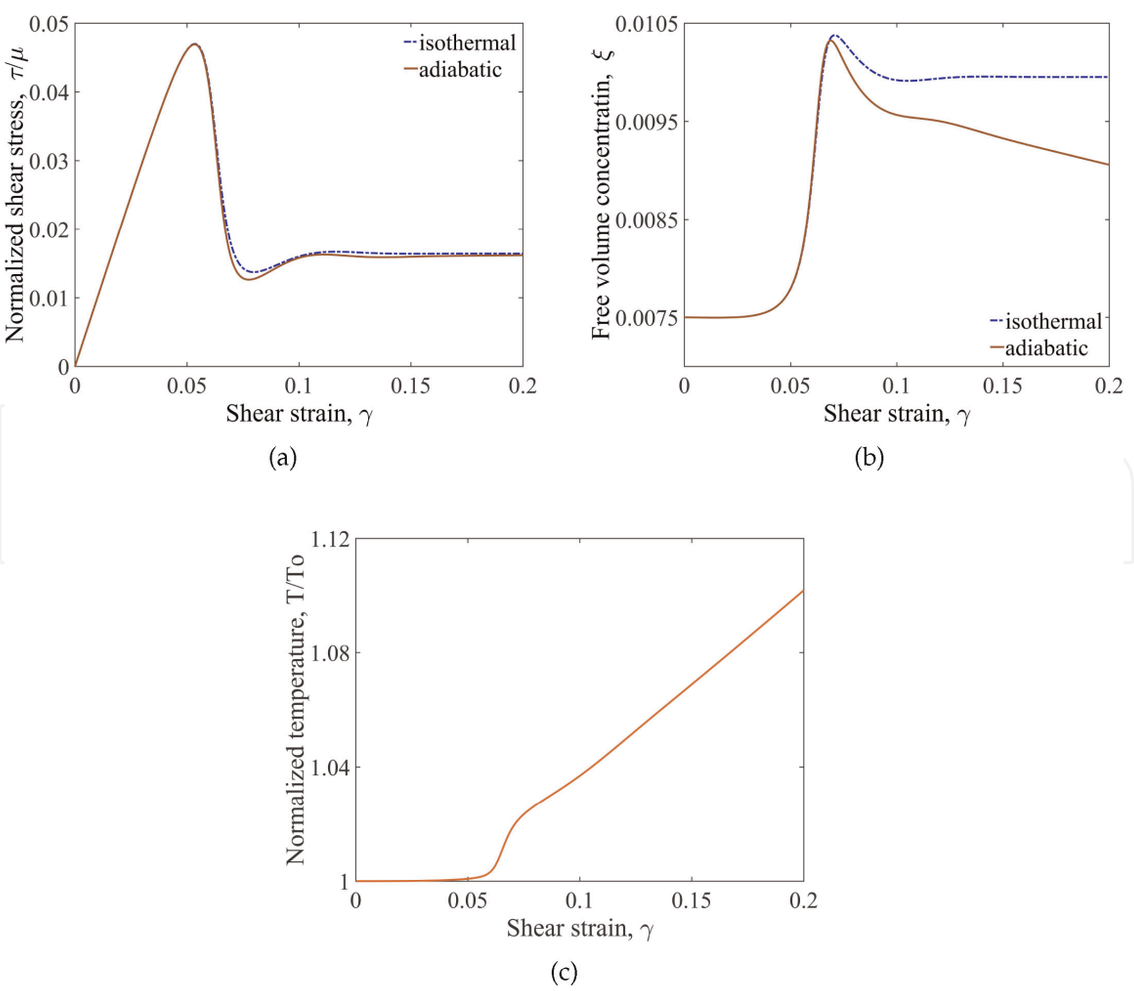

Figure 3.
Results for 1D shear problem for adiabatic homogeneous deformation. (a) Normalized shear stress versus shear strain, (b) free volume concentration versus shear strain and (c) normalized temperature versus shear strain.

creates more free volume and after some point, strain softening behavior occurs. In the meantime, temperature increases rapidly as plastic work is done. The normalized temperature increase is plotted against shear strain in **Figure 3c**. This instantaneous temperature rise lowers the energy barrier and hence helps in shear band nucleation. After a sharp turn in shear stress, it acquires a steady state. On the other hand, the temperature keeps rising steadily which promotes annihilation of free volume causing a continuous decrease in free volume concentration.

The main difference in the homogeneous isothermal model and adiabatic model is that in the isothermal model free volume remains constant after some point wherein the adiabatic model it keeps on decreasing. This is due to temperature change which helps in the annihilation process and hence free volume decreases. Shear stress after steady state is nearly the same in both the models.

3.3 Isothermal inhomogeneous deformation

In homogeneous case, the initial free volume is assumed to be uniform through the width, but in practical cases, this will never happen. There will be always some disturbance in free volume due to quenching or thermal fluctuations. Therefore in this section, it is assumed that initial free volume has some non-uniformity over the width of the strip.

For simplicity, finite amplitude disturbance in the form of Gaussian distribution is assumed. This disturbance is added to initially assumed free volume concentration [21]. So to get,

$$\xi(x, 0) = \xi_i + \delta \exp\left[-\frac{(x - x_0)^2}{\Delta^2}\right] \tag{38}$$

where ξ_i is initially assumed free volume which is constant, δ is amplitude of disturbance, x_0 is location where this disturbance is going to add and Δ is characteristic half width. Now for following case parameters are taken as, $\xi_i = 0.0075$, $\delta = 0.001$, $x_0 = 0$, $\Delta = 100l$ and $h = 2000l$ [21]. As x_0 is zero means disturbance will get added at midpoint of strip. Also it is assumed that $\Delta \ll h$ so that there will be very small effect of disturbance on the both boundaries and that can be neglected. All stresses and strains are assumed to be zero initially.

In inhomogeneous deformation normal stress will not be zero so effective shear stress will come into picture. Therefore Eqs. (24)–(27) should be solved simultaneously for variation of shear stress, normal stress, normal strain and free volume concentration, respectively. After normalization equations are,

$$\frac{\partial \xi}{\partial \hat{t}} = \frac{\partial^2 \xi}{\partial \hat{x}^2} + \exp\left(-\frac{\alpha}{\xi}\right)\left[\frac{\alpha}{\beta \overline{\mu} \xi}\{\cosh(\hat{\tau}_e \overline{\mu}) - 1\} - \frac{1}{n_D}\right] \tag{39}$$

$$\frac{d\hat{\tau}}{d\hat{t}} = \frac{r}{R} - \frac{1}{(h/l)} \int_{-h/l}^{h/l} \exp\left(-\frac{\alpha}{\xi}\right) \sinh(\hat{\tau}_e \overline{\mu}) \frac{\hat{\tau}}{\hat{\tau}_e} d\hat{x} \tag{40}$$

$$\frac{d\varepsilon}{d\hat{t}} = \frac{1}{(6h/l)} \int_{-h/l}^{h/l} \left[\exp\left(-\frac{\alpha}{\xi}\right) \sinh(\hat{\tau}_e \overline{\mu}) \frac{\hat{\sigma}}{\hat{\tau}_e} + \frac{\partial \xi}{\partial \hat{t}}\right] d\hat{x} \tag{41}$$

$$\frac{d\varepsilon}{d\hat{t}} = \frac{(1 - 2\nu)}{2\mu} \frac{\partial \sigma}{\partial \hat{t}} + \exp\left(-\frac{\alpha}{\xi}\right) \sinh(\hat{\tau}_e \overline{\mu}) \frac{\hat{\sigma}}{3\hat{\tau}_e} + \frac{1}{3} \frac{\partial \xi}{\partial \hat{t}} \tag{42}$$

Equation (39) is firstly converted into set of ordinary differential equations by using finite elements. Then all four equations are converted into algebraic equations using explicit method for time marching [46]. For explicit time marching method it is necessary to take very small time step, due to which computational time increases drastically. Integration with respect to x is carried out using modified trapezoidal rule. As there is negligible effect of disturbance in free volume at both boundaries and free volume is uniformly distributed near boundaries so it is assumed that, $\partial\xi/\partial x = 0$ at both boundaries. Shear strain is calculated from Eq. (21) at each time step.

Results shown in **Figure 4** are for different time steps where time is indicated by an average shear strain rate. **Figure 4a** shows a variation of free volume concentration over normalized distance means the width of the plate, while **Figure 4b** and **c** shows a variation of shear strain and normalized normal stress, respectively. **Figure 5** shows the variation of normalized shear stress with respect to shear strain. In the initial stage, shear stress is very small, therefore free volume change occurs due to only diffusion and annihilation processes. As these processes tend to decrease the free volume, initially amplitude of disturbance of free volume concentration decreases. Hence deformation is elastic and tends to be nearly homogeneous. But with time shear stress increases and free volume start to increase due to the stress-driven creation process. After some time the creation process of the free volume becomes more dominating than diffusion and annihilation. At that time amplitude of disturbance starts to grow. As it is seen in **Figure 4a** free volume concentration

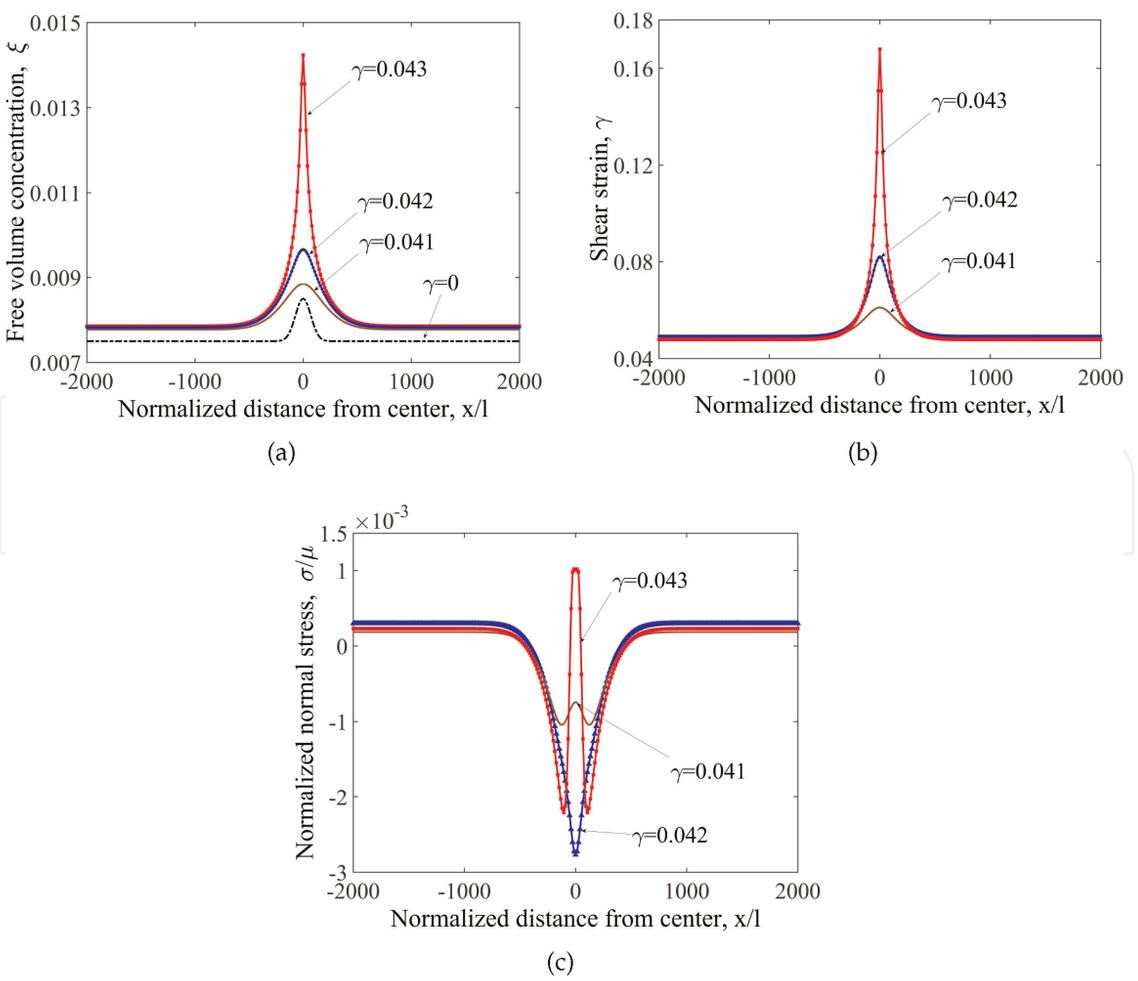

Figure 4.
Results for 1D shear problem with isothermal inhomogeneous deformation. Figure shows variation of (a) free volume concentration, (b) shear strain and (c) normalized normal stress over the normalized distance.

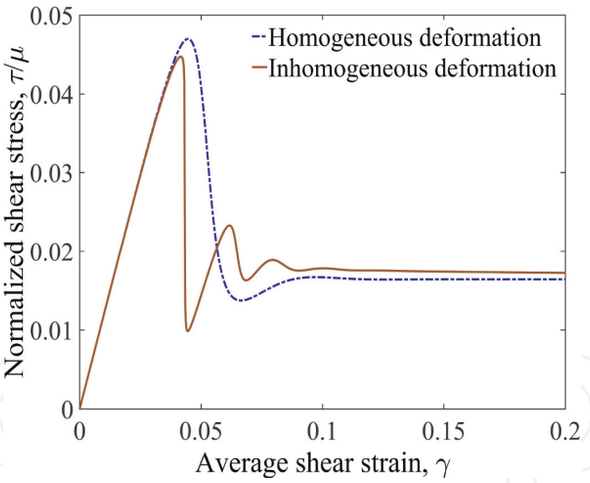

Figure 5.
Variation of shear stress for isothermal inhomogeneous deformation.

grows rapidly at the center of the disturbance. Meanwhile, shear strain increases rapidly where free volume concentration is increased, i.e., at the center of a plate, but decreases at the other locations as shown in **Figure 4b**. This develops inhomogeneous deformation in a plate. From **Figure 4c**, it can be seen that there is a drop in normal stress at the center but then it spikes up due to this inhomogeneous growth of free volume concentration. Here normal stress is smaller than shear stress. When there is instantaneous growth in free volume concentration shear stress falls abruptly as seen from **Figure 5**. But as shear stress falls, again creation process gets retarded and diffusion and annihilation processes dominate. This tends to reduce the localization effect. Eventually, the steady state is achieved where there is no variation in shear stress with respect to time.

The dashed line in **Figure 5** represents the normalized shear stress of homogeneous deformation solution. Initially, both solutions are nearly the same, but there is a difference after the peak value of shear stress is reached. Shear stress falls abruptly in case of inhomogeneous deformation due to an instantaneous increase in free volume concentration which is not the case for homogeneous deformation. Finally, inhomogeneous deformation gets converted into homogeneous deformation when the distribution of free volume becomes uniform. All results are very sensitive to several parameters like α, or initial free volume concentration.

3.4 Adiabatic inhomogeneous deformation

In this section inhomogeneous deformation is modeled as adiabatic process. As it is clear from Section 3.2 temperature also affects creation of shear bands and have influence on softening it is must to consider its effect in case of inhomogeneous deformation. Now again considering Eq. (24)–(28) and by normalizing them accordingly,

$$\frac{\partial \xi}{\partial \hat{t}} = \exp\left(-\frac{\Delta G^m}{k_B T_0 \hat{T}}\right)\exp\left(\frac{\Delta G^m}{k_B T_0}\right)\left[\frac{\partial^2 \xi}{\partial \hat{x}^2} + \exp\left(-\frac{\alpha}{\xi}\right)\left\{\frac{\alpha \hat{T}}{\beta \overline{\mu} \xi}\left\{\cosh\left(\frac{\hat{\tau}\overline{\mu}}{\hat{T}}\right) - 1\right\} - \frac{1}{n_D}\right\}\right] \tag{43}$$

$$\frac{d\hat{\tau}}{d\hat{t}} = \frac{1}{\vartheta_0}\exp\left(\frac{\Delta G^m}{k_B T_0}\right)\left[r - \frac{1}{2(h/l)}\int_{-h/l}^{h/l} 2\vartheta_0 \exp\left(-\frac{\alpha}{\xi}\right)\exp\left(-\frac{\Delta G^m}{k_B T_0 \hat{T}}\right)\sinh\left(\frac{\hat{\tau}\overline{\mu}}{\hat{T}}\right)\frac{\hat{\tau}}{\hat{\tau}_e} d\hat{x}\right] \tag{44}$$

$$\frac{d\varepsilon}{d\hat{t}} = \exp\left(\frac{\Delta G^m}{k_B T_0}\right)\frac{1}{(6h/l)}\int_{-h/l}^{h/l}\left[\exp\left(-\frac{\alpha}{\xi}\right)\exp\left(-\frac{\Delta G^m}{k_B T_0 \hat{T}}\right)\sinh\left(\frac{\hat{\tau}\overline{\mu}}{\hat{T}}\right)\frac{\hat{\sigma}}{\hat{\tau}_e}\right.$$

$$\left.+\exp\left(-\frac{\Delta G^m}{k_B T_0 \hat{T}}\right)\frac{\partial\xi}{\partial\hat{t}}\right]d\hat{x} \tag{45}$$

$$\frac{\partial\hat{\sigma}}{\partial\hat{t}} = \frac{2}{(1-2\nu)}\left[\frac{\partial\varepsilon}{\partial\hat{t}} - \frac{1}{3}\frac{\partial\xi}{\partial\hat{t}} - \frac{1}{3}\exp\left(-\frac{\Delta G^m}{k_B T_0 \hat{T}}\right)\exp\left(\frac{\Delta G^m}{k_B T_0}\right)\exp\left(-\frac{\alpha}{\xi}\right)\sinh\left(\frac{\hat{\tau}\overline{\mu}}{\hat{T}}\right)\frac{\hat{\sigma}}{\hat{\tau}_e}\right] \tag{46}$$

$$\frac{d\hat{T}}{d\hat{t}} = \exp\left(\frac{\Delta G^m}{k_B T_0}\right)\left[\frac{k}{\rho C_p \vartheta_0 l^2}\frac{\partial^2\hat{T}}{\partial\hat{x}^2} + \frac{2\mu}{T_0}\frac{\alpha_{TQ}\hat{\tau}}{\rho C_p}\exp\left(-\frac{\alpha}{\xi}\right)\exp\left(-\frac{\Delta G^m}{k_B T_0 \hat{T}}\right)\sinh\left(\frac{\hat{\tau}\overline{\mu}}{\hat{T}}\right)\right]$$

$$+\frac{2\mu}{T_0}\frac{\alpha_{TQ}\hat{\sigma}}{\rho C_p}\frac{\partial\varepsilon^p}{\partial\hat{t}} \tag{47}$$

Equations (43)–(47) are again solved by finite element method by using explicit time marching scheme. Boundary conditions are same for free volume concentration as mentioned in isothermal inhomogeneous case and for temperature similar boundary conditions are assumed as, $\partial T/\partial x = 0$ at both boundaries.

Figure 6 shows solution for adiabatic inhomogeneous case solved by explicit method with same parameters as used in earlier section. **Figure 6a** shows the distribution of free volume at different time steps, which are indicated by average shear strain. **Figure 6b–d** shows the distribution of normalized temperature, shear strain and the normalized normal stress, respectively.

As it is clear from previous sections initially when stress is low material is in an elastic state so the temperature remains almost constant. Free volume concentration initially decreases due to annihilation but then shoots up when stress increases with time. At the same time temperature inside the shear band increases very rapidly and can reach glass transition temperature. As initially, the temperature was uniform throughout the width it can be said that local heating must be caused due to increases in free volume. The temperature outside the shear band almost remains the same. This increase in free volume also softens the material causing the shear strain to increase in shear band region. But, as temperature increases suddenly annihilation process dominates over the creation process and large drop in free volume concentration is observed inside the shear band. Although free volume concentration drops, shear strain still increases as it depends on temperature also. Value of normalized normal stress shows a large increase in value near shear band but still, a pattern is the same as observed in the isothermal inhomogeneous case.

As shown in **Figure 7** due to softening shear stress value drops abruptly which leads to a decrease in free volume concentration even more as the creation process gets retarded. For elastic region results matches exactly with an isothermal inhomogeneous case as the temperature remains same until plastic work is done. As the temperature keeps on increasing which leads to more drop in free volume concentration. After some point, free volume concentration value inside the shear band goes below than the value of free volume concentration outside the shear band as shown in **Figure 8**. This inhomogeneity in free volume cannot be removed as the generation process is retarded and annihilation process is in favor of inhomogeneity. Which results in a continuous decrease in shear stress value and steady state is not achieved. Still, shear strain is accommodated in the shear band as temperature increases to very high value.

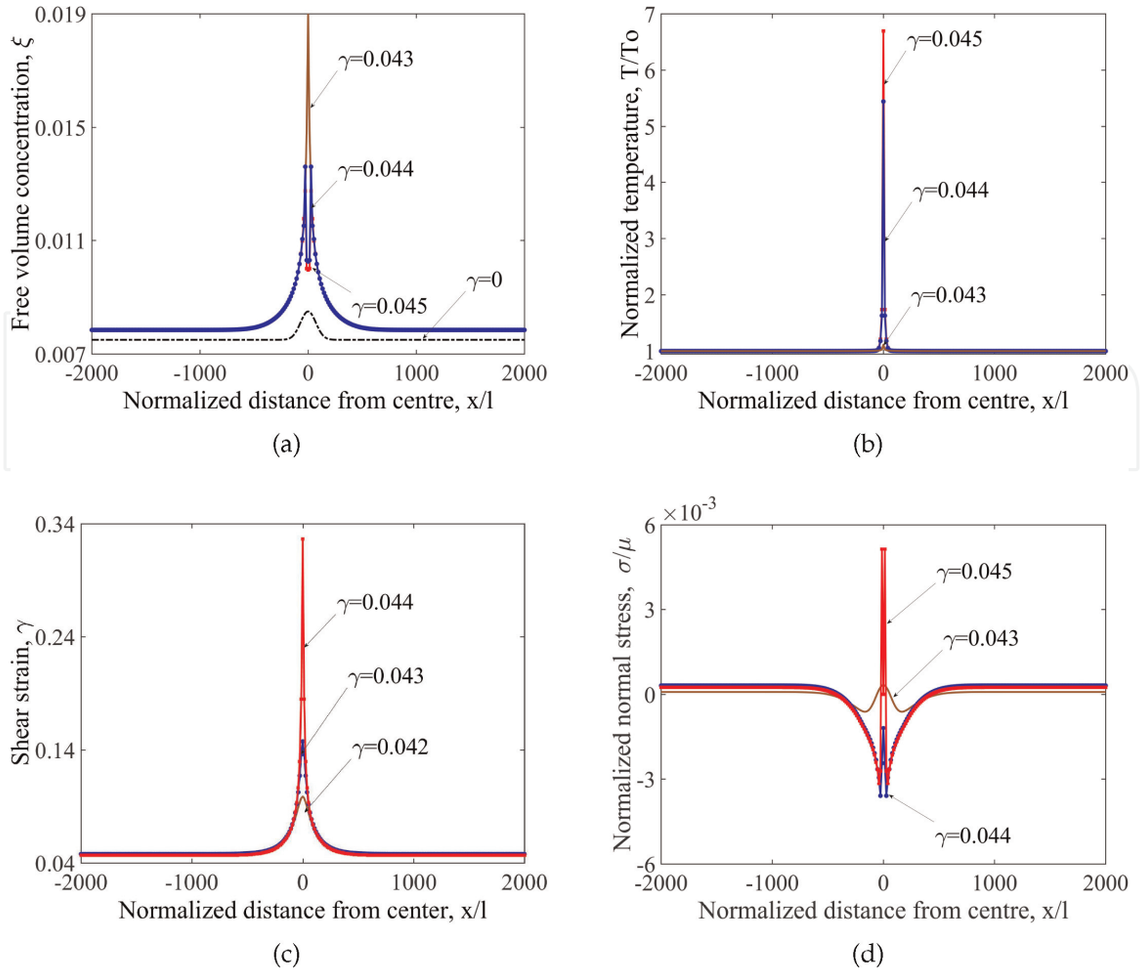

Figure 6.
Results for 1D shear problem with adiabatic inhomogeneous deformation. Figure shows variation of (a) free volume concentration, (b) normalized temperature, (c) shear strain and (d) normalized normal stress over the normalized distance.

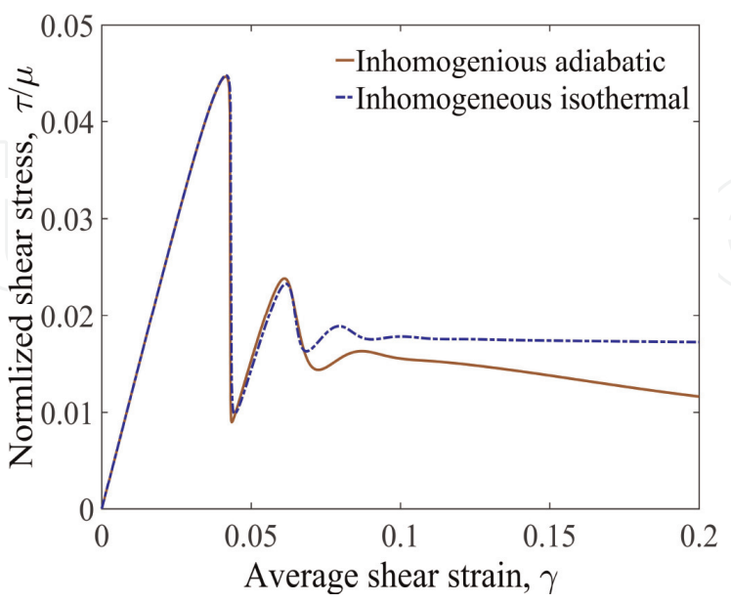

Figure 7.
Variation of shear stress for inhomogeneous adiabatic deformation.

These results fairly match with results obtained by Jiang and Dai [29], where the shear band is treated as an initial narrow zone of increased free volume concentration compared to the matrix surrounding it. This allows reduction of the governing

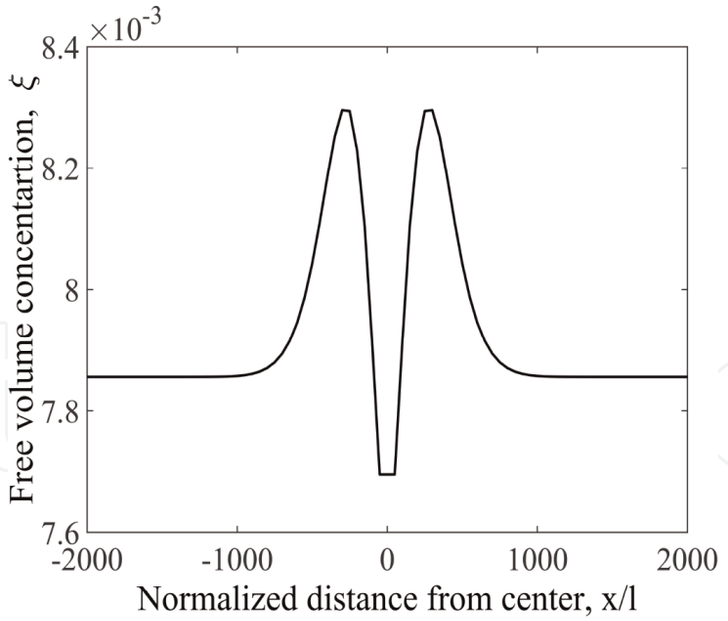

Figure 8.
Increased inhomogeneity in free volume concentration.

partial differential equations as a set of coupled ordinary differential equations which can be numerically integrated relatively easily. But the major issue with the approach adopted by Jiang and Dai [29] is that it can only be applied to the 1D problem whereas the approach used in present work can be readily extended to non-homogeneous solution in two/three dimensions [23].

4. Parametric study

All the parameters used to solve the 1D shear problem in previous sections were obtained by literature review for the sake of comparison with existing results. Parameters selected are influenced by work of Huang et al. [21], Gao et al. [28] and Jiang and Dai [29]. Results are very sensitive to several parameters. In this section, it is tried to study and understand how results will alter if there is a change in some parameters. It is found that there are many number of parameters to which results are very sensitive like geometrical factor α, an initial value of free volume concentration ξ_i, shear strain rate r, surrounding temperature (in most cases room temperature) T_0, etc. To keep the parametric study within the scope of this chapter, the effect of only two parameters is studied, namely: shear strain rate r and surrounding temperature T_0.

Figure 9 shows solution for isothermal homogeneous deformation case with initial free volume concentration as 0.008 for different values of applied shear strain rate. **Figure 9a** shows a variation of normalized shear stress with respect to shear strain while **Figure 9b** shows a variation of free volume concentration. From **Figure 9** it is seen that as the value of applied shear strain rate increases maximum value attained by shear stress also increases. This is due to the fact that as shear strain rate is increased there is less time for annihilation process to decrease the free volume and as stress increases rapidly large amount of free volume gets generated. This increased free volume later causes the softening. Steady state value of shear stress is not much affected by this change of shear strain rate but a steady state value of free volume concentration decreases as strain rate decreases. If the strain rate is very low then the rate of generation of free volume never exceeds the rate of

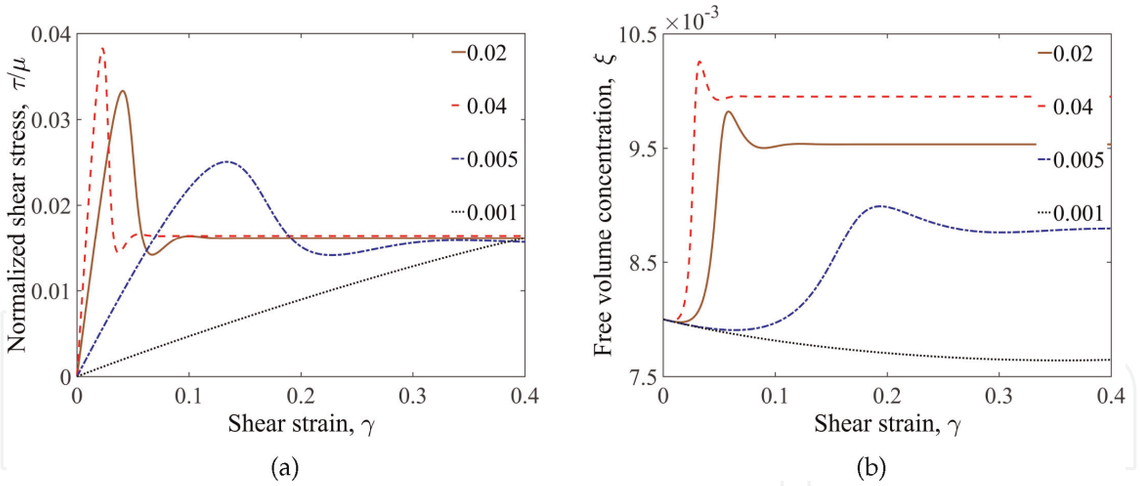

Figure 9.
Solution for isothermal homogeneous deformation case with various applied shear strain rates. (a) Normalized shear stress versus shear strain, and (b) free volume concentration versus shear strain.

the annihilation of free volume hence free volume always keeps on decreasing and softening does not occur at all.

Figure 10 shows solution for isothermal homogeneous deformation case with initial free volume concentration as 0.008 for different values of surrounding temperature. **Figure 10a** shows a variation of normalized shear stress with respect to shear strain while **Figure 10b** shows a variation of free volume concentration. From **Figure 10**, it can be seen that initially when shear strain is very low all the solutions match with each other. As surrounding temperature increases it supports annihilation process and hence free volume concentration decreases. But this decrease in free volume delays the softening and therefore maximum value of shear stress increases. Again this increased shear stress produces more and more free volume by dominating over annihilation process and hence the maximum value of free volume concentration is more in case of maximum surrounding temperature. In this case, also after softening steady state is achieved but values are different for different surrounding temperature. A similar effect will be seen in the case of inhomogeneous deformation. In the case of adiabatic deformation effect of change of applied strain rate will be similar but the effect of change of surrounding temperature may vary by some amount.

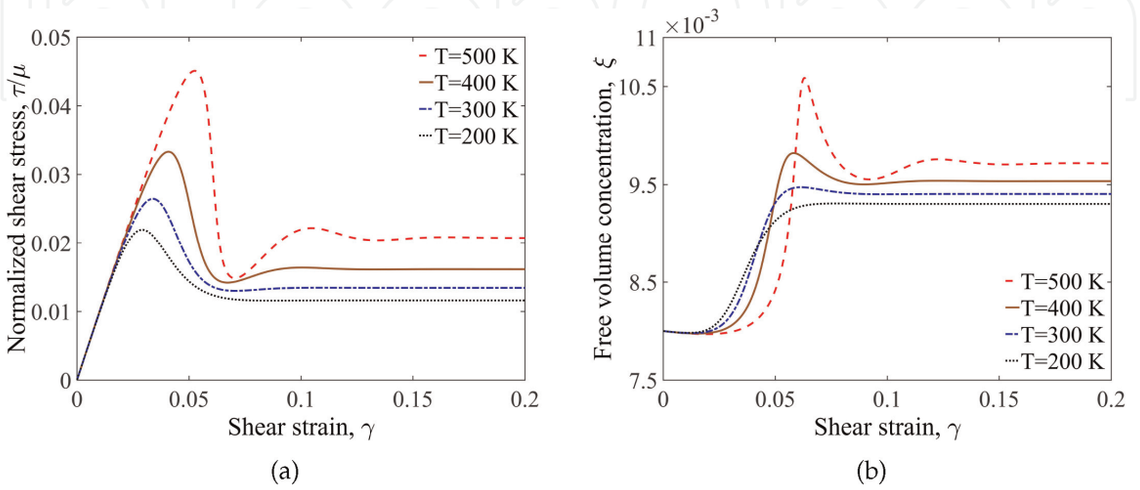

Figure 10.
Solution for isothermal homogeneous deformation case with various surrounding temperatures. (a) Normalized shear stress versus shear strain, and (b) free volume concentration versus shear strain.

As seen in this section solution varies drastically with the change in parameters, therefore a selection of parameters should be done very carefully.

5. Conclusions

This chapter presents a theoretical framework for modeling of shear band formation in homogeneous and inhomogeneous deformation in MGs by considering shear banding process as an adiabatic process and adopting free volume as an order parameter. A problem of infinitely long thin strip undergoing shear strain is solved for four different scenarios namely: (1) homogeneous isothermal, (2) homogeneous adiabatic, (3) inhomogeneous isothermal and (4) inhomogeneous adiabatic deformation, undergoing infinitesimal deformation.

Shear bands observed in case of MGs can be modeled by using free volume theory effectively. When shear banding is considered as an adiabatic process temperature keeps on increasing and therefore free volume concentration keeps on reducing as annihilation process dominates due to increased temperature. Hence, although the assumption of shear banding process as isothermal process reduces the complexity of theory considerably but still effect of temperature should also be considered as it is an important parameter and alters result by a large amount. In homogeneous case MG always attain a steady state where shear stress does not vary with time and MG flows like a liquid. When free volume concentration is not uniform throughout the material which is the most practical case, inhomogeneity grows to cause the formation of the shear band where free volume concentration is higher initially. Shear strain inside shear band grows rapidly and can reach a critical value of strain which may cause crack initiation leading to full fracture.

Acknowledgements

The author greatly acknowledges the guidance of Prof. Tanmay K. Bhandakkar from Indian Institute of Technology of Bombay, Mumbai, India. This work would not be possible without the helpful discussions with him.

Abbreviations

MGs	metallic glasses
BMGs	bulk metallic glasses
STZ	shear transformation zone
1D	one-dimensional
2D	two-dimensional
ODE	ordinary differential equation
PDE	partial differential equation

IntechOpen

Author details

Shank S. Kulkarni
The University of North Carolina at Charlotte, Charlotte, USA

*Address all correspondence to: skulka17@uncc.edu;
shankkulkarni1316@gmail.com

References

[1] Turnbull D. Formation of crystal nuclei in liquid metals. Journal of Applied Physics. 1950;**21**(10):1022-1028

[2] Turnbull D, Cech RE. Microscopic observation of the solidification of small metal droplets. Journal of Applied Physics. 1950;**21**(8):804-810

[3] Jun WK, Willens RH, Duwez PO. Non-crystalline structure in solidified gold-silicon alloys. Nature. 1960; **187**(4740):869

[4] Telford M. The case for bulk metallic glass. Materials Today. 2004;**7**(3):36-43

[5] Ashby MF, Greer AL. Metallic glasses as structural materials. Scripta Materialia. 2006;**54**(3):321-326

[6] Xu J, Ramamurty U, Ma E. The fracture toughness of bulk metallic glasses. JOM. 2010;**62**(4):10-18

[7] Lewandowski JJ, Wang WH, Greer AL. Intrinsic plasticity or brittleness of metallic glasses. Philosophical Magazine Letters. 2005; **85**(2):77-87

[8] Murali P, Guo TF, Zhang YW, Narasimhan R, Li Y, Gao HJ. Atomic scale fluctuations govern brittle fracture and cavitation behavior in metallic glasses. Physical Review Letters. 2011; **107**(21):215501

[9] Gilman JJ. Flow via dislocations in ideal glasses. Journal of Applied Physics. 1973;**44**(2):675-679

[10] Gilman JJ. Mechanical behavior of metallic glasses. Journal of Applied Physics. 1975;**46**(4):1625-1633

[11] Chaudhari P, Levi A, Steinhardt P. Edge and screw dislocations in an amorphous solid. Physical Review Letters. 1979;**43**(20):1517

[12] Shi LT. Dislocation-like defects in an amorphous Lennard-Jones solid. Materials Science and Engineering. 1986;**81**:509-514

[13] Takeuchi S, Edagawa K. Atomistic simulation and modeling of localized shear deformation in metallic glasses. Progress in Materials Science. 2011; **56**(6):785-816

[14] Argon AS. Plastic deformation in metallic glasses. Acta Metallurgica. 1979; **27**(1):47-58

[15] Cohen MH, Turnbull D. Molecular transport in liquids and glasses. The Journal of Chemical Physics. 1959;**31**(5): 1164-1169

[16] Polk DE, Turnbull D. Flow of melt and glass forms of metallic alloys. Acta Metallurgica. 1972;**20**(4):493-498

[17] Spaepen F. A microscopic mechanism for steady state inhomogeneous flow in metallic glasses. Acta Metallurgica. 1977;**25**(4):407-415

[18] Taub AI, Spaepen F. The kinematics of structural relaxation of metallic glass. Acta Metallurgica. 1980;**28**(12):1781-1788

[19] Steif P, Spaepen F, Hutchinson J. Strain localization in amorphous metals. Acta Metallurgica. 1982;**30**(2):447-449

[20] Vaks VG. Possible mechanism for formation of localized shear bands in amorphous alloys. Physics Letters A. 1991;**159**(3):174-178

[21] Huang R, Suo Z, Prevost JH, Nix WD. Inhomogeneous deformation in metallic glasses. Journal of the Mechanics and Physics of Solids. 2002; **50**(5):1011-1027

[22] Kulkarni SS, Bhandakkar TK. Study of the effect of large deformation

through a finite deformation based constitutive model for metallic glasses. In: ASME 2018 International Mechanical Engineering Congress and Exposition; American Society of Mechanical Engineers; 2018. pp. V009T12A010-V009T12A010

[23] Gao YF. An implicit finite element method for simulating inhomogeneous deformation and shear bands of amorphous alloys based on the free-volume model. Modelling and Simulation in Materials Science and Engineering. 2006;**14**(8):1329

[24] De Hey P, Sietsma J, Van Den Beukel A. Structural disordering in amorphous Pd40Ni40P20 induced by high temperature deformation. Acta Materialia. 1998;**46**(16):5873-5882

[25] Yang B, Liaw PK, Wang G, Morrison M, Liu CT, Buchanan RA, et al. In-situ thermographic observation of mechanical damage in bulk-metallic glasses during fatigue and tensile experiments. Intermetallics. 2004;**12**(10–11):1265-1274

[26] Yang B, Liu CT, Nieh TG, Morrison ML, Liaw PK, Buchanan RA. Localized heating and fracture criterion for bulk metallic glasses. Journal of Materials Research. 2006;**21**(4):915-922

[27] Lewandowski JJ, Greer AL. Temperature rise at shear bands in metallic glasses. Nature Materials. 2006; **5**(1):15

[28] Gao YF, Yang B, Nieh TG. Thermomechanical instability analysis of inhomogeneous deformation in amorphous alloys. Acta Materialia. 2007;**55**(7):2319-2327

[29] Jiang MQ, Dai LH. On the origin of shear banding instability in metallic glasses. Journal of the Mechanics and Physics of Solids. 2009;**57**(8):1267-1292

[30] Ruan HH, Zhang LC, Lu J. A new constitutive model for shear banding instability in metallic glass. International Journal of Solids and Structures. 2011;**48**(21):3112-3127

[31] Conner RD, Johnson WL, Paton NE, Nix WD. Shear bands and cracking of metallic glass plates in bending. Journal of Applied Physics. 2003;**94**(2):904-911

[32] Ravichandran G, Molinari A. Analysis of shear banding in metallic glasses under bending. Acta Materialia. 2005;**53**(15):4087-4095

[33] Dasgupta R, Hentschel HG, Procaccia I. Microscopic mechanism of shear bands in amorphous solids. Physical Review Letters. 2012;**109**(25): 255502

[34] Singh I, Guo TF, Murali P, Narasimhan R, Zhang YW, Gao HJ. Cavitation in materials with distributed weak zones: Implications on the origin of brittle fracture in metallic glasses. Journal of the Mechanics and Physics of Solids. 2013;**61**(4):1047-1064

[35] Huang X, Ling Z, Dai LH. Cavitation instabilities in bulk metallic glasses. International Journal of Solids and Structures. 2013;**50**(9):1364-1372

[36] Schuh CA, Hufnagel TC, Ramamurty U. Mechanical behavior of amorphous alloys. Acta Materialia. 2007;**55**(12):4067-4109

[37] Greer AL, Cheng YQ, Ma E. Shear bands in metallic glasses. Materials Science & Engineering R: Reports. 2013; **74**(4):71-132

[38] Timoshenko SP. Strength of Materials. New York: D. Van Nostrand Company; 1955

[39] Khan AS, Huang S. Continuum Theory of Plasticity. New York: John Wiley and Sons; 1995

[40] Yavari AR, Pang S, Louzguine-Luzgin DV, Inoue A, Lupu N, Nikolov N, et al. Change in thermal expansion coefficient of bulk metallic glasses Tg measured by real-time diffraction using high-energy synchrotron light. Journal of Metastable and Nanocrystalline Materials. 2003;**15**: 105-110

[41] Kato H, Chen HS, Inoue A. Relationship between thermal expansion coefficient and glass transition temperature in metallic glasses. Scripta Materialia. 2008;**58**(12): 1106-1109

[42] Spaepen F. Metallic glasses: Must shear bands be hot? Nature Materials. 2006;**5**(1):7

[43] Kulkarni SS, Bhandakkar TK. Thermo-mechanical model for inhomogeneous deformations in metallic glasses. Computer Aided Engineering. 2013:446-451

[44] Kulkarni SS. Modelling of shear bands in metallic glasses. Indian Institute of Technology Bombay. 2013

[45] Reddy JN. An Introduction to the Finite Element Method. New York: McGraw-Hill; 1993

[46] Hutton D. Fundamentals of Finite Element Analysis. New York: McGraw-Hill; 2004